Optik - International Journal for Light and Electron Optics 272 (2023) 170216

Contents lists available at ScienceDirect

Optik

journal homepage: www.elsevier.com/locate/ijleo

Gadolinium-tungsten-boron trioxide glasses: A multi-phase research on cross-sections, attenuation coefficients, build-up factors and individual transmission factors using MCNPX

Ghada ALMisned [a], Duygu Sen Baykal [b,*], Fatema T. Ali [c], Ghaida Bilal [d], G. Kilic [e], H.O. Tekin [d,f,**]

[a] Department of Physics, College of Science, Princess Nourah Bint Abdulrahman University, P.O. Box 84428, Riyadh 11671, Saudi Arabia
[b] Istanbul Kent University, Vocational School of Health Sciences, Medical Imaging Techniques, Istanbul 34433, Turkey
[c] Center for Advanced Materials Research (CAMR), Research Institute of Sciences and Engineering, University of Sharjah, Sharjah 27272, United Arab Emirates
[d] Department of Medical Diagnostic Imaging, College of Health Sciences, University of Sharjah, 27272 Sharjah, United Arab Emirates
[e] Eskisehir Osmangazi University, Faculty of Science, Department of Physics, Eskişehir, Turkey
[f] Istinye University, Faculty of Engineering and Natural Sciences, Computer Engineering Department, Istanbul 34396, Turkey

ARTICLE INFO

Keywords:
Gadolinium oxide glasses
Phy-X/PSD
MCNPX
Radiation shielding

ABSTRACT

The oxide of the rare earth element gadolinium has the chemical formula Gd_2O_3. Also known as gadolinium sesquioxide, gadolinium trioxide, and Gadolinia, gadolinium oxide. In this study, various types of fundamental cross-sections, attenuation coefficients, build-up factors and individual transmission factors of high density gadolinium-tungsten-boron trioxide glasses with a chemical composition of (70-x)WO_3-xGd_2O_3 –30B_2O_3 (where x: 17.5, 20.0, 22.5, 25.0 and 27.5 mol%) are determined using advanced Monte Carlo methods. In addition, gamma transmission factors (TFs) for a range of medical and industrial radioisotopes were calculated using MCNPX (version 2.7.0) Monte Carlo code. The investigated glasses were classified Gd17.5, Gd20.0, Gd22.5, Gd25.0, and Gd27.5 in accordance with xGd_2O_3. Our findings suggest that the Gd27.5 sample (with highest of Gd_2O_3 content mol. %) has possessed the maximum linear (μ) and mass (μ/ρ) attenuation coefficients at all gamma-ray energies investigated. The coded glass sample Gd27.5 is achieved the maximum effective atomic number (Z_{eff}) and effective electron density (N_{eff}) owing its superior attenuation properties. In terms of build-up factors, increasing the concentration of xGd_2O_3 in glasses is decreased the EBF and EABF values for all mean free path values (0.5–40 mfp). At a thickness of 3 cm, the lowest transmission factor (i.e., highest attenuation) was verified for all Gd17.5-Gd27.5 glasses investigated. Consequently, the Gd27.5 sample exhibits superior radiation shielding properties for a large range of photon energy and various medical and industrial radioisotope energies.

* Corresponding author.
** Corresponding author at: Department of Medical Diagnostic Imaging, College of Health Sciences, University of Sharjah, 27272 Sharjah, United Arab Emirates.
E-mail addresses: duygu.sen@kent.edu.tr (D. Sen Baykal), htekin@sharjah.ac.ae (H.O. Tekin).

https://doi.org/10.1016/j.ijleo.2022.170216
Received 18 September 2022; Accepted 8 November 2022
Available online 11 November 2022
0030-4026/© 2022 Elsevier GmbH. All rights reserved.

Table 1
Samples code, elemental weight fraction. density. and molar volume of WO_3-Gd_2O_3-B_2O_3: (x = 17.5, 20.0, 22.5, 25.0 and 27.5 mol% glasses).

Samples Code	Elemental weight fraction (wt%)				Density (g/cm^3)
	B	O	Gd	W	
Gd17.5	0.093171	0.338688	0.151828	0.416312	5.45
Gd20.0	0.093171	0.336822	0.173518	0.396488	5.55
Gd22.5	0.093171	0.334957	0.195208	0.376664	5.70
Gd25.0	0.093171	0.333092	0.216898	0.356839	5.85
Gd27.5	0.093171	0.331226	0.238588	0.337015	6.00

1. Introduction

There has been a rise in the number of research conducted on the radiation absorption characteristics of glass in recent years [1–5]. Numerous factors contribute to this phenomenon, but the exceptional structural characteristics of glass materials and their non-toxic, ecologically beneficial attributes are perhaps the most important [6,7]. The investigations include in-depth analyses of the attenuation qualities against not only gamma and x-rays, but also alpha [8,9], protons [10], and neutrons [11–15], which are all forms of particle radiation. Not surprisingly, gamma and x-ray radiation are two of the most useful forms of radiation for both medical and industrial purposes. This circumstance has prompted an increase in the intensity of the investigations by elevating the significance of the absorption characteristics of glass materials against such radiations. In contrast to other forms of radiation, such as alpha particles, x-ray and gamma-ray interacts with matter by ionization and is very penetrating due to its high frequency and presents an external threat [16]. Despite the many advantages and uses of gamma radiation, ionizing radiation, on the other hand, may cause damage to tissues and cells owing to its biological effects, such as chromosomal abnormalities and carcinogenic effects [16–18]. Cell damage is determined by the quantity of radiation received and the radiosensitivity of the exposed organ. Radiation dangers vary from immediate effects caused by high radiation doses to stochastic effects whose chance increases with exposure to radiation. ALARA was created to enhance radiation awareness and exposure avoidance. It is based on three guiding principles: decreasing exposure duration, increasing distance from the radiation source, and using shielding to decrease distributed radiation [19]. Medical personnel and patients are frequently shielded from direct and indirect radiation by radiation-shielding clothing. Lead and other metals such as tungsten, antimony, and barium are used to create radiation shields and protective clothing in a variety of forms and styles [20]. Previously, several working groups have examined the radiation shielding properties and application possibilities to increase radiation protection efficacy and optimize shield usage in activities [21–23]. Due to its transparency, ease of manufacture, thermal stability, high permeability, and mechanical properties, glass materials have lately emerged as viable options for a variety of applications. Due to the abovementioned considerations, scientists and engineers were interested in utilising glass materials as optical and radiation shielding facilities [24–26]. Glasses, being non-toxic materials that can be manufactured in high densities, have also been stressed and developed in routine radiation safety applications [27]. Meanwhile, Gd_2O_3 is one of the oxides that may be incorporated with B, O, Gd and W to form a glass structure [28,29]. To increase the neutron and radiation shielding qualities of glass compositions, tungsten trioxide oxide is added in varying amounts. The authors were compensated for their work studying the changes in mechanical, optical, and radiation attenuation properties that result from varying Gd_2O_3 additive concentrations in group (70-x)WO_3-xGd_2O_3 –30B_2O_3 (where x is 17.5, 20.0, 22.5, 25.0 and 27.5 mol%), which studied before for 225–662 keV narrow energy range [30]. By expanding the concept of gamma-ray attenuation parameters given in the study and additionally calculating some new parameters such as transmission (TF) and build-up factors, it is aimed to better understand the structures of these glasses towards providing a larger scale data for those promising glass samples. The outcomes of the current research may provide some useful information on the role of tungsten trioxide in the production and design of radiation protective glass materials.

2. Materials and methods

2.1. Glass materials

From earlier reference [30], five samples of gadolinium-tungten-boron trioxide with chemical formula (70-x)WO_3-xGd_2O_3 –30B_2O_3 (where x is 17.5, 20.0, 22.5, 25.0 and 27.5 mol%), were chosen. The studied glasses were formulated and named as follows:

Gd17.5: 0.093171B+ 0.338688 O+ 0.151828Gd+ 0.416312 W with density (ρ = 5.45 g/cm^3).
Gd20.0:0.093171B+ 0.336822 O+ 0.173518Gd+ 0.396488 W with density (ρ = 5.55 g/cm^3).
Gd22.5:0.093171B+ 0.334957 O+ 0.195208Gd+ 0.376664 W with density (ρ = 5.70 g/cm^3).
Gd25.0:0.093171B+ 0.333092 O+ 0.216898Gd+ 0.356839 W with density (ρ = 5.85 g/cm^3).
Gd27.5:0.093171B+ 0.331226 O+ 0.238588Gd+ 0.337015 W with density (ρ = 6.00 g/cm^3).

In Table 1, each glass sample's density, code, and percentage of elemental weight are listed.

2.2. Studied parameters

As a measure of the photon absorption by the material, the linear attenuation coefficients (LAC) of the materials are examined. To properly shield materials from radiation, it is required to study the LAC, which represents the probability of all photon interactions,

photoelectric events, Compton scattering, and pair creation events. The LAC provides the chance of any contact per photon unit length [31]:

$$I(x) = I_o e^{-\mu x} \tag{1}$$

Where is the probability of total interaction per unit thickness in a shield material, the linear attenuation coefficient (μ) is given as, with units of cm^{-1}. (where; I and I_0 represent the incoming and attenuated gamma ray intensity and t is the mass thickness of the sample.) By dividing the LAC by the specific gravity of the material, one can calculate the mass attenuation coefficient (MAC). The mass attenuation coefficient (MAC) is defined as the rate at which the beam is attenuated per unit mass and is denoted by the symbol x [32].

$$\mu_m = \frac{\mu}{\rho} \tag{2}$$

The useful thickness that allows the intensity of radiation traveling through a target to reduce to half by interacting with the material is referred to as the half-value layer (HVL, $X_{1/2}$) and is denoted by the formula [33];

$$X_{1/2} = \frac{\ln(2)}{\mu} \tag{3}$$

On the other hand, tenth value layer ($X_{1/10}$) is the material thickness required to reduce the primary radiation count value by one tenth; it is expressed in centimeters and represented by [31,32]:

$$X_{1/10} = \frac{\ln(10)}{\mu} \tag{4}$$

Another of the shielding characteristics, the mean free path (MFP) is described by the following formula as the distance a particle travels before probable collisions with other particles [32].

$$mfp = \frac{1}{\mu} \tag{5}$$

The composite's effective atomic number is influenced by the Compton scattering interaction process and may be determined using the following formula [32,33]:

$$Z_{eff} = \frac{\sigma_T}{\sigma_e} \tag{6}$$

In addition, there is a linear connection between the effective atomic number (N_{eff}) and the electron density [34].

$$N_{eff} = N_A \frac{Z_{eff}}{< A_{eff} >} \quad \left(\frac{electrons}{g}\right) \tag{7}$$

ACS (σ_T) denotes the likelihood of interactions between primary photons and composite atoms and is a function of the mass attenuation coefficient (μ/ρ) [31–34]:

$$\sigma_T = \left(\frac{\sum_i f_i A_i}{N_A}\right) \cdot \left(\frac{\mu}{\rho}\right) barns \Big/ atom\ or\ cm^2 \Big/ g \tag{8}$$

N_A:Avogadro's number.
$\sum_i f_i A_i$:Atomic mass of the compound.
A_i:Atomic mass of the i_{th} element.
F_i:Mole fraction of the i_{th} element.
The ECS (σ_e) is a measure of the frequency at which elementary photons and composite electrons interact [31–34]:

$$\sigma_e = \left(\frac{1}{N_A}\right) \sum_i \left[\frac{f_i A_i}{Z_i}\left(\frac{\mu}{\rho}\right)\right] barns \Big/ atom\ or\ cm^2 \Big/ g \tag{9}$$

Where Z_i is the atomic number of i_{th} element. The buildup factor comprises the response of non-colliding photons and the contribution of scattered photons. The exposure buildup factor (EBF) is a parameter linked to the amount of absorption or stored energy in the air; this parameter dictates the degree to which a source and detector may interact in the air. Different compounds have distinct energy absorption and accumulation factors (EABF). This is the quantity of energy absorbed by the material with which the radiation interacts [31–34]. In the current study, all radiation shielding parameters (μ, μ_m,$X_{1/2}$, $X_{1/10}$, mfp, Z_{eff},N_{eff}, σ_T, σ_e,EBF and EABF) were assessed using the Phy-X/PSD program [35].

2.3. Calculation of transmission factor (TF) values through MCNPX code

The transmission properties of materials in the presence of primary ionizing radiation must be considered in the assessment of materials that will be employed in radiation fields. Because the transmission factor (TF) is a characteristic of gamma-ray attenuation

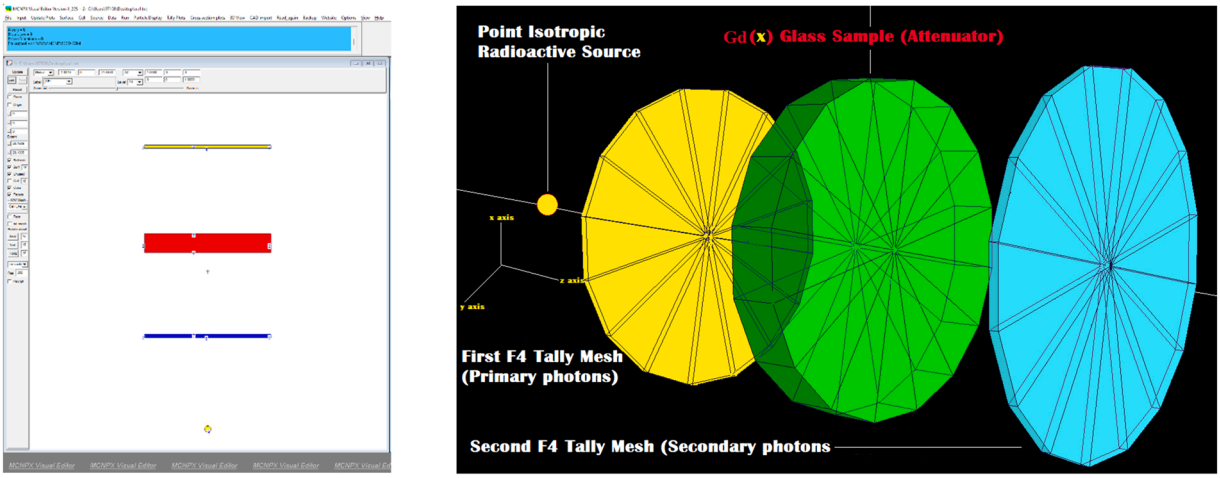

Fig. 1. **(a)** 2-D view of designed MCNPX simulation setup **(b)** 3-D illustration of designed MCNPX setup (2-D and 3-D views are obtained from MCNPX Visual Editor VisedX22S).

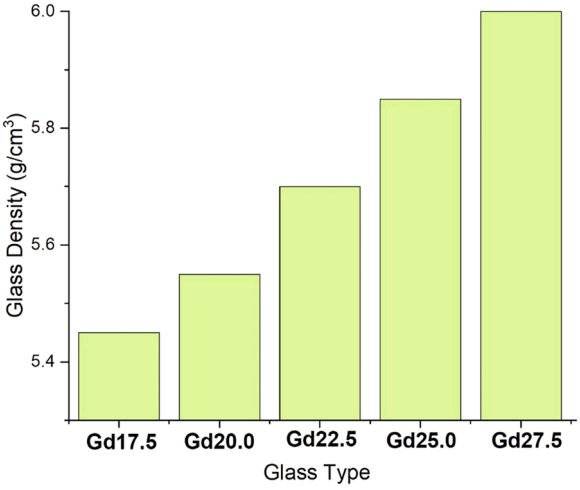

Fig. 2. Variation of glass densities (g/cm^3).

that provides considerable assessment possibilities, it is used as a specialized evaluation measure by researchers. In this study, the TFs of glasses (Gd17.5 - Gd27.5) comprised of B, O, Gd and W with different chemical compositions were comprehensively calculated and evaluated utilizing several assessment criteria. In addition to TFs, the Phy-X/PSD algorithm also calculated and behaviorally examined other critical gamma-ray shielding factors in the 0.015–15 MeV photon energy range. Using the well-known radiation transport algorithm MCNPX, we estimated TFs for a broad range of radioisotopes as follows ^{67}Ga-^{57}Co-^{111}In-^{133}Ba-^{201}Tl-$^{99\,m}$Tc-^{51}Cr-^{131}I–^{58}Co-^{137}Cs-^{60}Co. Intensities of primary and secondary gamma radiation are measured by detector sections positioned in front of and behind the glass barrier, respectively. The MCNPX [36] simulation setup used to compute the gamma-ray transmission factor is shown in Fig. 1. Typically, the first step in the creation of a proper input file for Monte Carlo simulation applications is to collect all the variables such as geometrical properties of the tools, material definitions of the tools, source definition, source distribution that represent the overall simulation environment. The elemental percentage distributions (wt%) and densities given for each glass sample are the two most essential components in the final input file [36]. A material's precise attenuation capabilities in the presence of both primary and secondary gamma rays must be evaluated in addition to its fundamental gamma-ray shielding qualities. This technique has the potential to provide useful data on the amount of gamma rays that penetrated the shield. A better understanding of the attenuation capabilities of shielding materials against ionizing gamma rays may be possible if one calculates these quantities using the transmission factor, which is a basic measure (TF). In this study, MCNPX (version 2.7.0) Monte Carlo simulation code has been utilized in order to calculate the transmission factor (TF) of the glasses that were examined. The transmission factor (TF) of the absorber was calculated by comparing the amount of radiation that was absorbed by its surface to the amount that was absorbed by its material

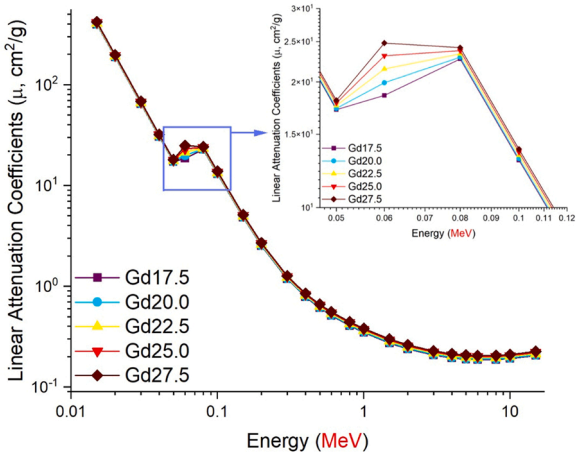

Fig. 3. : Variations of linear attenuation coefficient (cm^{-1}) with photon energy (MeV) for all S1-S6 glasses.

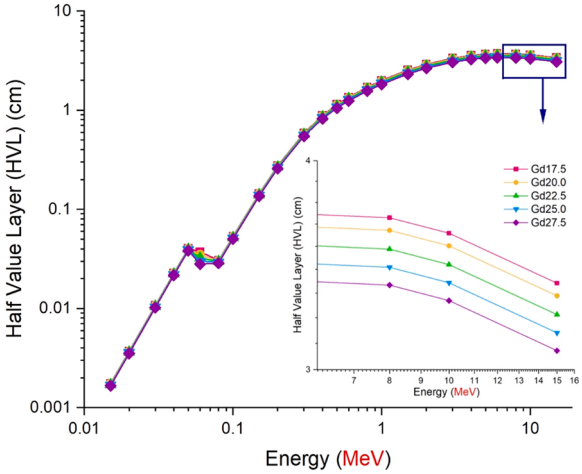

Fig. 4. Variations of half value layer (cm) with photon energy (MeV) for all S1-S6 glasses.

medium. To determine the TF of the glasses that we examined, we multiplied the average gamma-ray flux that was detected in the F4 tally mesh by the average gamma-ray flux that was detected in the uniform detection field. To implement this idea in MCNPX code, we first had to build up a pair of detecting areas (see Fig. 1) in front of and behind the glass sample. In the detecting ring in front of the glass material, the intensity of primary gamma rays was measured, and in the detecting ring behind the glass material, the intensity of attenuated gamma rays that passed through the glass was detected [36].

3. Results and discussions

The basic shielding features of five different glass samples based on the WO_3-Gd_2O_3-B_2O_3 system against ionizing gamma rays with energy between 0.015 and 15 MeV were examined. Fig. 2 depicts the variation of glass densities for Gd17.5, Gd20.0, Gd22.5, Gd25.0 and Gd27.5, respectively. Glasses, as may be observed, have densities between 5.45 and 6.00 g/cm^3. The density of the glass has grown to 0.55 g/cm3 due to the addition of 10 mol% Gd_2O_3. The primary goal of this research is to highlight the effects of the above-mentioned density increase on the fundamental gamma-ray attenuation qualities and unique TFs of each glass sample. Initially, a key density-dependent gamma-ray shielding factor, the linear attenuation coefficient, was then determined (cm^{-1}). The percentage of photons in a monoenergetic beam that are attenuated per unit thickness may be expressed in terms of a constant metric called the linear attenuation coefficient (μ). Increases in both atomic number and physical density of the absorbing substance led to larger linear attenuation coefficients. Fig. 3 depicts the variation of μ values as a function of the energy of incoming gamma rays. The values' attitude changed with respect to the gamma-ray energy band, as was apparent. The In the low-energy zone, μ values were decreased noticeably because of the photoelectric effect's primacy. Although the decline was still most apparent in the mid-energy range, the dominance of Compton Scattering ensured that the degree of the reduction became less sudden over time. The highest linear attenuation coefficient values across the board were found for the Gd27.5 sample. Nonetheless, the findings showed that in the high energy

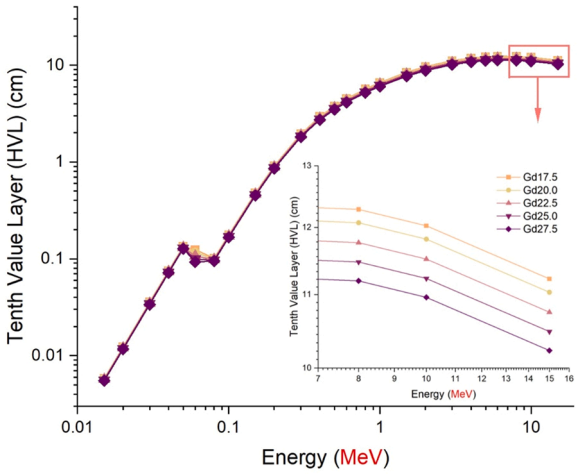

Fig. 5. Variations of tenth value layer (cm) with photon energy (MeV) for all S1-S6 glasses.

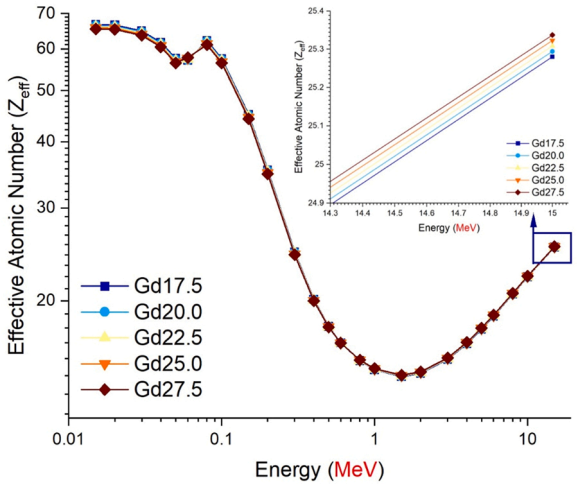

Fig. 6. Variations of effective atomic number (Z_{eff}) with photon energy (MeV) for all S1-S6 glasses.

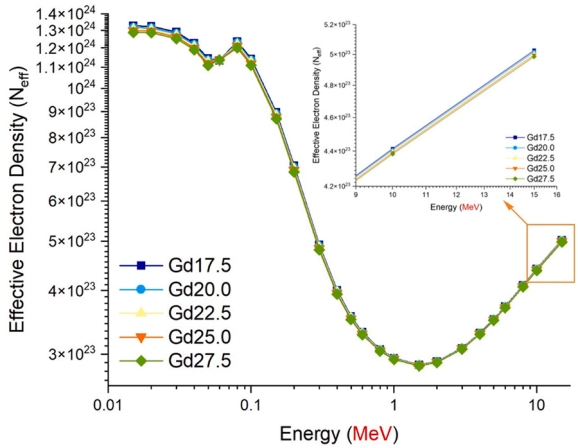

Fig. 7. Variations of effective electron density (electrons/g) with photon energy (MeV) for all S1-S6 glasses.

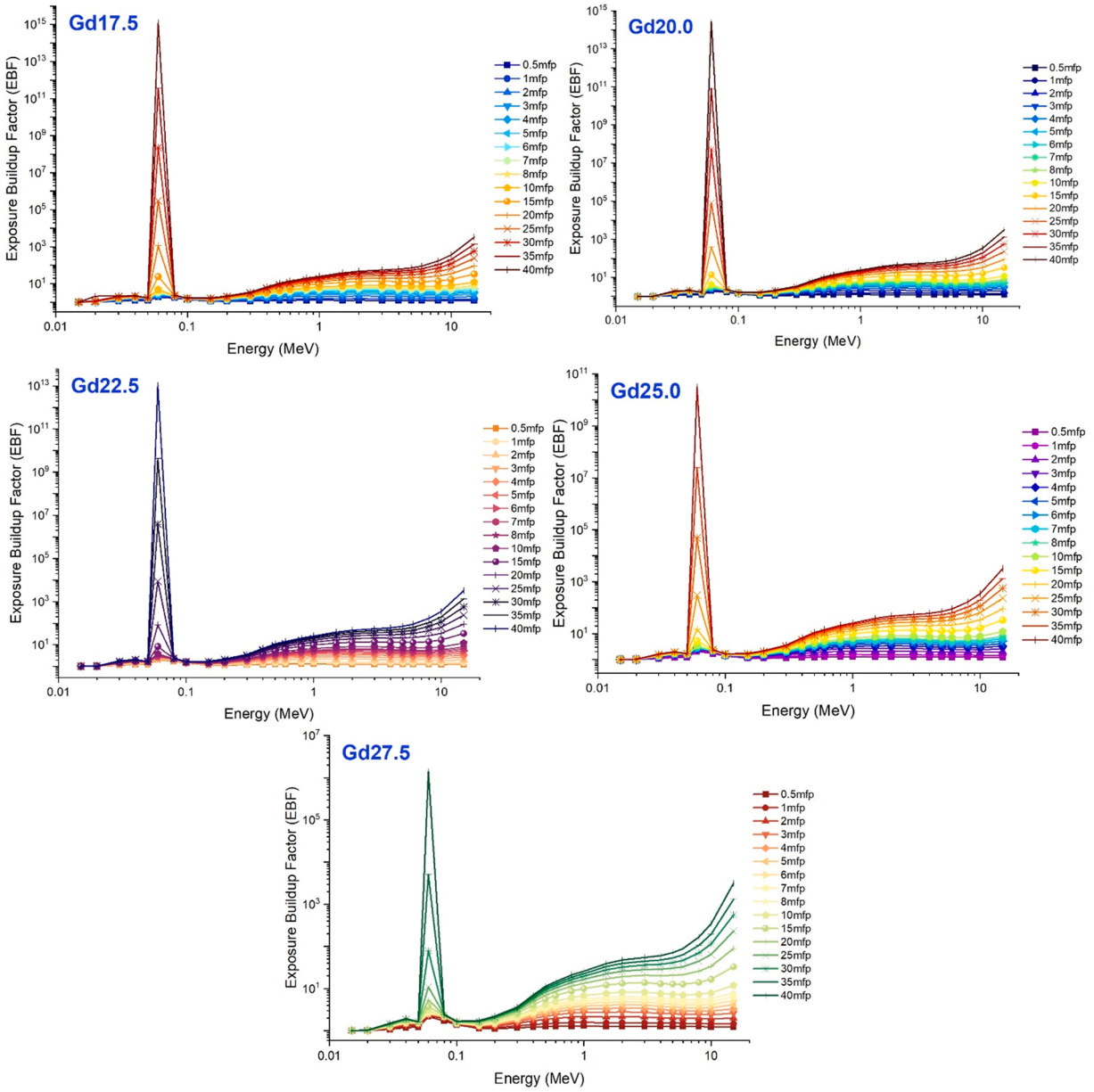

Fig. 8. : Variation of exposure buildup factors (EBF) of investigated glasses at different mean free path values.

range, there were no variations among the analysed samples. Due to the adaptability of glass composition, the average density difference between Gd17.5 and Gd27.5 samples is just 0.55 g/cm^3. In nuclear and medical radiation applications, the tenth value layer (TVL, $X_{1/10}$) is a crucial parameter, and its calculation provides extremely relevant and practically applicable data for determining the shielding material's sufficiency. Like the half-value layer (HVL, $X_{1/2}$), seen in Fig. 4, the (TVL, $X_{1/10}$) may be utilized to provide an additional parameter that is also function-related. This figure specifies the thickness of the material necessary to reduce the radiation intensity on the material by a factor of ten. Fig. 5 depicts the variation in thickness by a factor of energy for the heavy metal oxide glasses that were tested. Values in the tenth layer are more than twice as large as those in the half layer for the same energy levels. This is to be expected, and more robust shielding material is needed to reduce the radiation intensity by a certain amount, perhaps, to one tenth. The investigation showed that the Gd27.5 sample has the lowest values for thickness at the one-tenth value, even though these two parameters have different quantitative values for the same energy values. Based on these two characteristics, it has been shown that the Gd27.5 sample would provide minimum required material thicknesses in any procedure using photon energy between 0.015 and 15 MeV. Once radiation has made first interaction with and penetrated the inner areas of the shielding material, individual photons may interact with the atoms of the shielding material. When the energy of the incoming radiation is reduced to zero due to

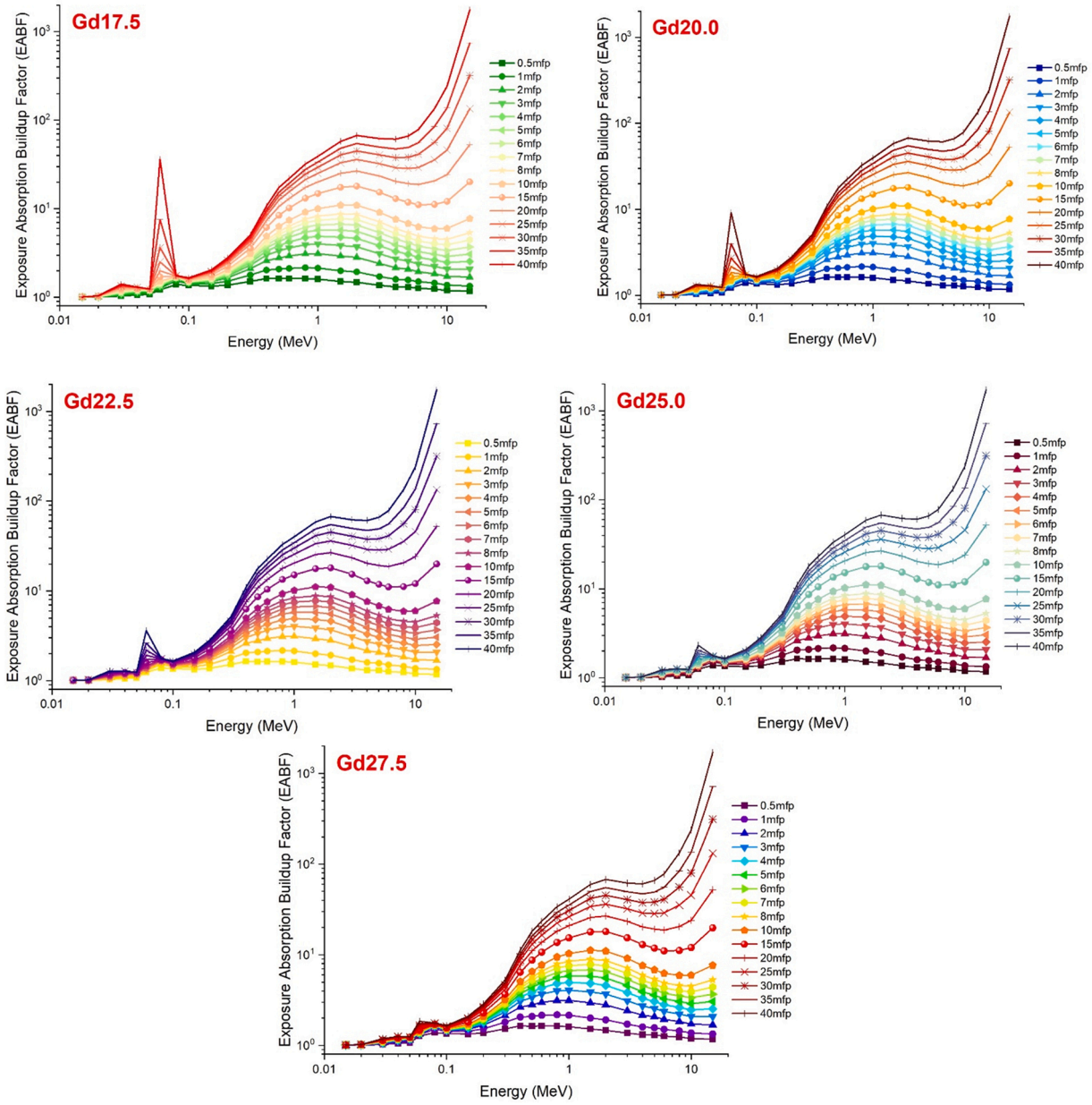

Fig. 9. : Variation of energy absorption buildup factors (EABF) of investigated glasses at different mean free path values.

these interactions, it is completely absorbed. The probability of gamma-ray energy loss due to interactions with the electrons of the atoms is affected by the atomic number and, by extension, the number of electrons in the atom's orbits. Z_{eff} and N_{eff} values for the studied (Gd17.5 - Gd27.5) glasses were determined with the use of Eqs. (5–6). The effective atomic number (Z_{eff}) and effective electron density (N_{eff}) as a function of photon energy are shown in Fig. 6 and Fig. 7. The highest Z_{eff} values are seen in the low-energy region yet, there is a high probability for photoelectric interaction mechanism. Meanwhile, Z_{eff} was found to significantly increase in the lowest energy range of this behaviour, with the increase in Z_{Gd}= 64 in the glass matrix being responsible for most of the increase. Our results showed that the Gd27.5 sample has the highest N_{eff} and Z_{eff} values within the investigated energy range. Thus, the Gd27.5 sample would have the largest atomic number and, consequently, the maximum electron density during the attenuation of the incoming gamma rays. For mean free path values between 0.5 and 40 mfp, Figs. 8–9 displays the exposure build-up factor (EBF) and the energy absorption build-up factor (EABF) as a function of energy (MeV). Large increases in these values are seen at photon energies of 0.04 MeV, 0.06 MeV, 0.08 MeV, 0.1 MeV, and 15 MeV, all following a similar trend. However, increases in EBF and EABF values are more noticeable at greater energy intensities up to 15 MeV, and they grow rather gradually at shallower penetration depths. For denser materials and a wider range of incident x-rays or gamma rays, higher mfp values generally lead to photon accumulation. Our research

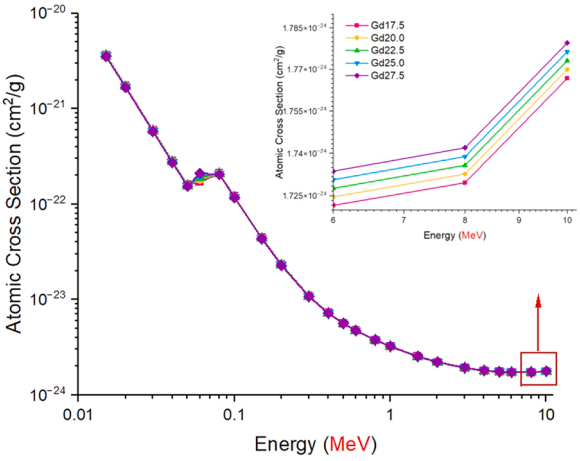

Fig. 10. Variations of atomic cross section with photon energy (MeV) for all S1-S6 glasses.

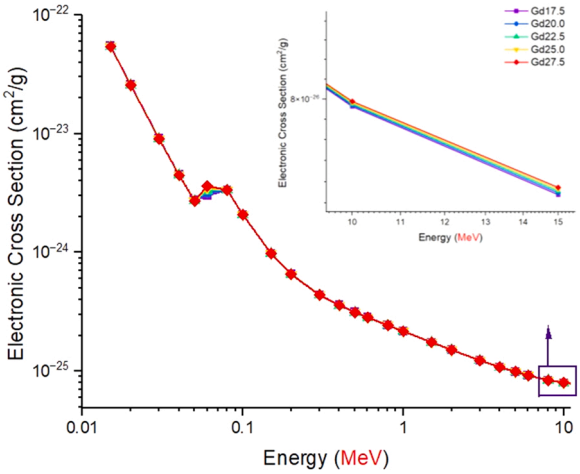

Fig. 11. Variations of electronic cross section with photon energy (MeV) for all S1-S6 glasses.

indicates that the Gd27.5 sample, which has excellent attenuation capabilities against gamma rays, has the lowest feasible EBF and EABF values. Determining the radiation shielding parameters ACS and ECS allows one to calculate the effective atomic number (Z_{eff}) of the studied glasses. Variation in ACS as a function of incoming photon energy is shown in Fig. 10, whereas variation in ECS is shown in Fig. 11. Figs. 10 and 11 show that as photon energy rises, the ACS and ECS values decrease. Also, for all glasses, the values of the ACS parameters are larger than the ECS values. This is because the chance of full atomic interaction with incoming photons is higher than the probability of complete electrical contact with any substance. Finally, gamma-ray transmission factor (TF) values for a variety of common radioisotope energies were calculated for glass samples made of Gd17.5, Gd20.0, Gd22.5, Gd25.0, and Gd27.5. TF values were calculated using two different methods. Glass of different thicknesses (Gd17.5, Gd20.0, Gd22.5, Gd25.0, and Gd27.5) were tested first for their TF factors. For reference, Fig. 12 shows the TFs of the glasses under study as a function of the radioisotope energy used (MeV) for a range of glass thicknesses. The transmission factor is shown to increase correspondingly when the radioisotope's energy goes up from 0.0086 MeV to 1.3325 MeV. It was found that the glass samples had the lowest TF values across the board in the low energy area. This is because low-energy gamma rays are very effectively absorbed by these relatively thick samples. Nonetheless, at around 0.1 MeV, a clear split becomes apparent. Different glass thicknesses react differently to incoming gamma rays after 0.1 MeV. The maximum attenuation (and lowest transmission) values were measured at a thickness of 3 centimetres for all glass types tested. In this case, the attenuation of entering gamma rays may be understood by considering the influence of shield thickness on the attenuation capabilities of any shielding material. The attenuation capabilities of the examined glasses were then compared over a range of glass thicknesses (0.5 cm, 1.5 cm, 2.5 cm, and 3 cm) to determine their TF values. Fig. 13 displays the relationship between the radioisotope energy (in MeV) and the transmission factors (TFs) for a range of glass thicknesses. Additionally, the lowest TF values for a glass thickness of 3 cm were supplied for all samples. Transmission was lowest for the Gd27.5 sample across all glass thicknesses tested. The basic shielding features of five different glass samples based on the WO_3-Gd_2O_3-B_2O_3 system against ionizing gamma rays with energy between 0.015 and 15 MeV were examined.

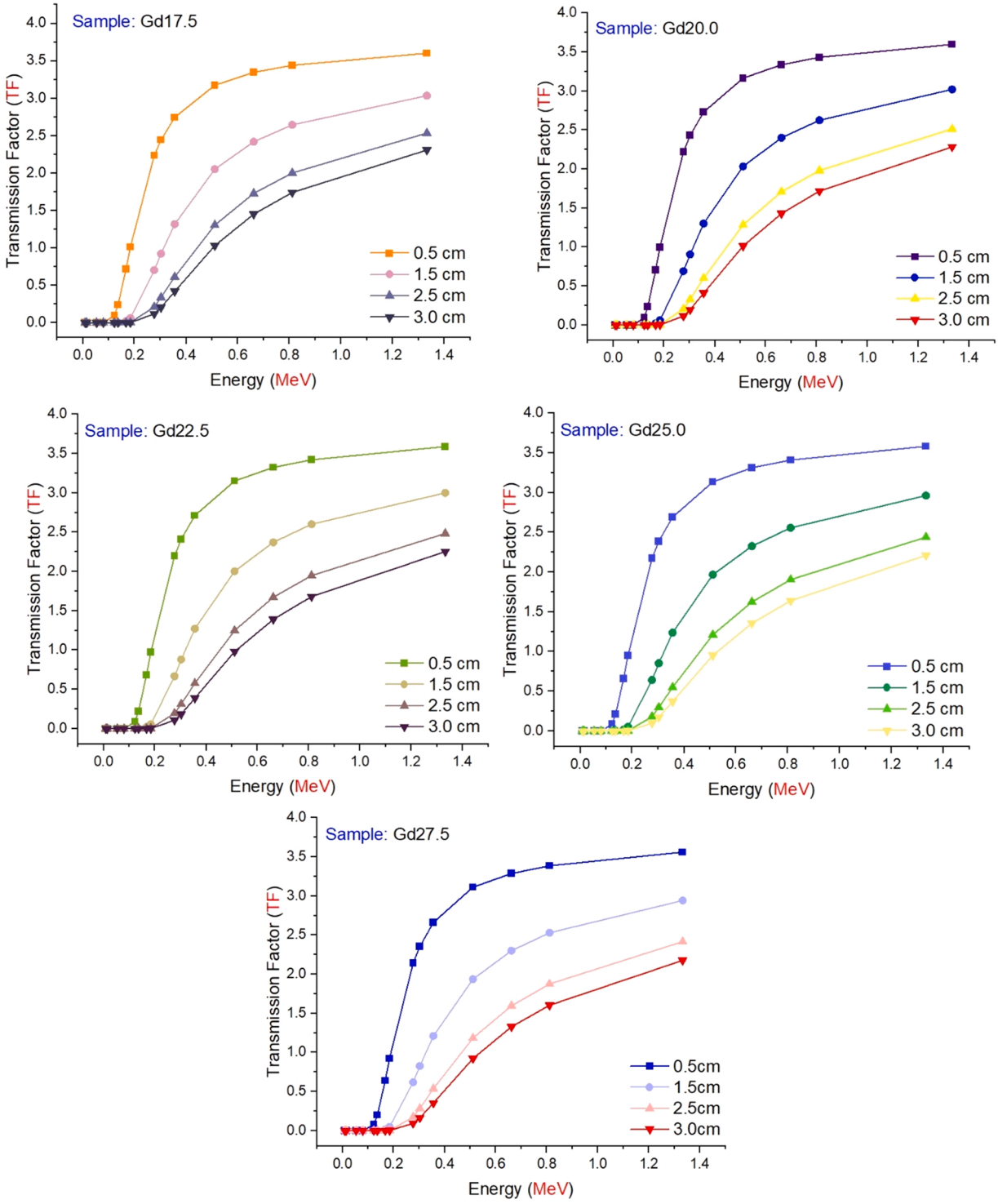

Fig. 12. : Transmission Factors (TFs) of investigated glasses as a function of used radioisotope energy (MeV) at different glass thicknesses.

4. Conclusion

The gamma-ray attenuation parameters as well as the transmission factors of high-density glasses comprised of sodium meta-phosphate, tungsten trioxide, and fixed antimony trioxide have been investigated. Gd_2O_3 has some promising applications such as special optical glass and plasma display panels, fluorescent materials, luminescence, and electroluminescent devices, UV detectors as

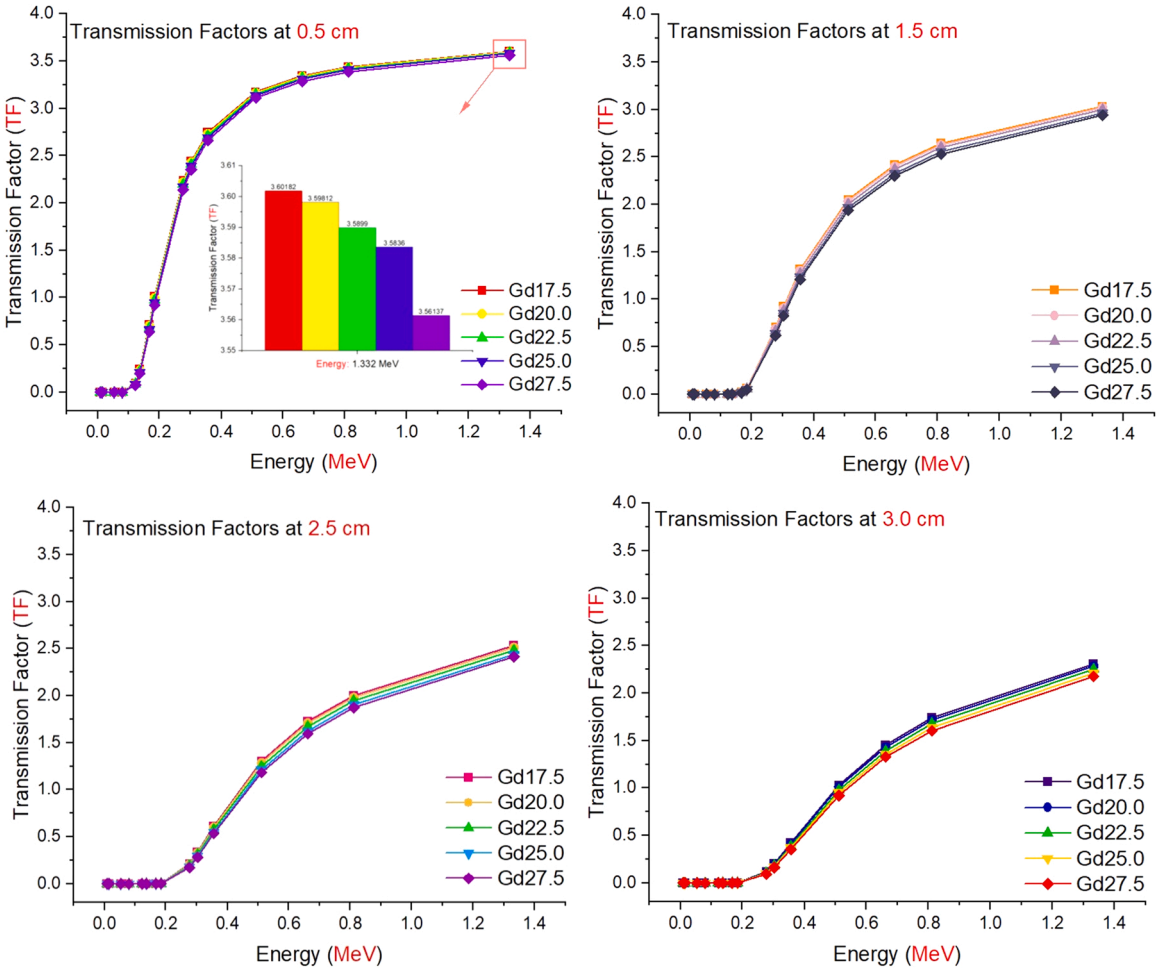

Fig. 13. : Comparison of the Transmission Factors (TFs) as a function of used radioisotope energy (MeV) for different glass thicknesses.

well as some bioimaging applications. Moreover, it`s significant properties have a broad-range applications for x-ray medical imaging with high-resolution, scintillators and sintering aids and neutron converters. These promising properties Gd_2O_3 has prompted us to extend the previously studied investigation by incorporating some non-studied gamma-ray properties as well as individual transmission factors. The findings may be applicable to the employment of these glasses in radiation and radiation-based applications, which was the primary motivation for the study. Following is a summary of the findings and key points of the current investigation.

- The Gd27.5 has the highest linear (μ) and mass (μ_m) attenuation coefficients.
- Linear (μ) and mass (μ_m) were validated by the following pattern: Gd17.5 $_{\mu,\ \mu/\rho}$ <Gd20.0 $_{\mu,\ \mu/\rho}$ <Gd22.5 $_{\mu,\ \mu/\rho}$ <Gd25.0 $_{\mu,\ \mu/\rho}$ <Gd27.5 $_{\mu,\ \mu/\rho}$.
- Gd27.5 has achieved the minimum values of Half (HVL) and tenth (TVL) layers
- The effective atomic number (Z_{eff}) and effective electron density (N_{eff}) of the investigated glasses follow the same pattern as LAC and MAC.
- Increasing the concentration of xGd_2O_3 in glasses decreased the EBF and EABF values for all mean free path values (0.5–40 mfp).
- As the radioisotope energy rises from 0.0086 MeV to 1.3325 MeV, the transmission factor (TF) increases proportionally.
- In the low energy region, the glass samples exhibited the lowest TF values for all thicknesses.
- At a thickness of 3 cm, the lowest transmission factor (highest attenuation) was verified for all Gd17.5-Gd27.5 glasses investigated. However, the Gd27.5 sample exhibits superior radiation shielding properties.

Results from this study demonstrate that Gd_2O_3 may be used as a powerful monotonic instrument for enhancing gamma-ray reduction parameters and boosting the protectiveness of transmission factors, as shown by the study's broad evaluation parameters. However, there may be a potential for the results to evolve to a more applicable level if the scientific community conducts studies to ensure the sustainability of these parameters in terms of application and considers various assessment ideas and existing results collectively.

Declaration of Competing Interest

None.

Data availability

Data will be made available on request.

Acknowledgements

None.

References

[1] M.I. Sayyed, H.O. Tekin, Malaa M. Taki, M.H.A. Mhareb, O. Agar, E. Sakar, Kawa M. Kaky, Bi2O3-B2O3-ZnO-BaO-Li2O glass system for gamma ray shielding applications, Optik 201 (2020), 163525, https://doi.org/10.1016/j.ijleo.2019.163525.

[2] S. Kaewjaeng, S. Kothan, N. Chanthima, H.J. Kim, J. Kaewkhao, Gamma radiation shielding materials of lanthanum calcium silicoborate glasses, Part 1, Mater. Today.: Proc. Volume 5 (Issue 7) (2018) 14901–14906, https://doi.org/10.1016/j.matpr.2018.04.027.

[3] R. Kurtulus, M.S. Buriahi, Shams A.M. Issa, H.O. Tekin, T. Kavas, E. Kavaz, Physical, structural, mechanical and radiation shielding features of waste pharmaceutical glasses doped with Bi2O3, Optik (2022), 169108, https://doi.org/10.1016/j.ijleo.2022.169108.

[4] G. Kilic, E. Ilik, Shams A.M. Issa, Ghada ALMisned, H.O. Tekin, Tailoring critical material properties of some ternary glasses through ZnO/CdO alteration: a focusing study on multiple behavioral changes, Appl. Phys. A 128 (2022) 890, https://doi.org/10.1007/s00339-022-06040-8.

[5] W. Cheewasukhanont, P. Limkitjaroenporn, S. Kaewjaeng, W. Chaiphaksa, W. Hongtong, J. Kaewkhao, Development of bismuth sodium borate glasses for radiation shielding material, Mater. Today.: Proc. Volume 43 (Part 3) (2021) 2508–2515, https://doi.org/10.1016/j.matpr.2020.04.610.

[6] Gokhan Kilic, Shams A.M. Issa, Erkan Ilik, O. Kilicoglu, U. Gokhan Issever, R. El-Mallawany, Bashar Issa, H.O. Tekin, Physical, thermal, optical, structural, and nuclear radiation shielding properties of Sm2O3 reinforced borotellurite glasses, Ceram. Int. 47 (2021) 6154–6168, https://doi.org/10.1016/j.ceramint.2020.10.194.

[7] Gokhan Kilic, Erkan Ilik, Shams A.M. Issa, Bashar Issa, M.S. Al-Buriahi, U.Gokhan Issever, Hesham M.H. Zakaly, H.O. Tekin, Ytterbium (III) oxide reinforced novel TeO2-B2O3-V2O5 glass system: synthesis and optical, structural, physical and thermal properties, Ceram. Int. 47 (2021) 18517–18531, https://doi.org/10.1016/j.ceramint.2021.03.175.

[8] U. Perişanoğlu, Assessment of nuclear shielding and alpha/proton mass stopping power properties of various metallic glasses, Appl. Phys. A 125 (2019) 801, https://doi.org/10.1007/s00339-019-3105-8.

[9] I.O. Olarinoye, F.I. El-Agawany, A. El-Adawy, El. Sayed Yousef, Y.S. Rammah, Mechanical features, alpha particles, photon, proton, and neutron interaction parameters of TeO2–V2O3–MoO3 semiconductor glasses, Ceram. Int. Volume 46 (Issue 14) (2020) 23134–23144, https://doi.org/10.1016/j.ceramint.2020.06.093.

[10] Ghada ALMisned, H.O. Tekin, Esra Kavaz, Ghaida Bilal, Shams A.M. Issa, Hesham M.H. Zakaly, Antoaneta Ene. Gamma, Fast Neutron, Proton, and Alpha Shielding Properties of Borate Glasses: A Closer Look on Lead (II) Oxide and Bismuth (III) Oxide Reinforcement, Appl. Sci. 11 (2021) 15, https://doi.org/10.3390/app11156837.

[11] E.F. El Agammy, A.M.A. Mostafa, M. Al-Zaibani, H.O. Tekin, R. Ramadan, Amr Essawy and Shams A.M. Issa. Tailoring the structuralism in xBaO·(30–x) $Li_2O·70B_2O_3$ glasses for highly efficient shields of Gamma radiation and neutrons attenuators, Phys. Scr. (2021) Accept. Manuscr. Online (2021), https://doi.org/10.1088/1402-4896/ac297b.

[12] G. Lakshminarayana, H.O. Tekin, M.G. Dong, M.S. Al-Buriahi, Dong-Eun Lee, Jonghun Yoon, Taejoon Park, Comparative assessment of fast and thermal neutrons and gamma radiation protection qualities combined with mechanical factors of different borate-based glass systems, Results Phys. 37 (2022), 105527, https://doi.org/10.1016/j.rinp.2022.105527.

[13] E. Kavaz, E. Ilik, G. Kilic, Ghada ALMisned, H.O. Tekin, Synthesis and experimental characterization on fast neutron and gamma-ray attenuation properties of high-dense and transparent Cadmium oxide (CdO) glasses for shielding purposes, Available online 10 May 2022, Ceram. Int. (2022), https://doi.org/10.1016/j.ceramint.2022.04.338.

[14] G. Kilic, E. Kavaz, E. Ilik, Ghada ALMisned, H.O. Tekin, CdO-rich quaternary tellurite glasses for nuclear safety purposes: Synthesis and experimental gamma-ray and neutron radiation assessment of high-density and transparent samples, Opt. Mater. 129 (2022), 112512, https://doi.org/10.1016/j.optmat.2022.112512.

[15] Hesham M.H. Zakaly, H.O. Tekin, Shams A.M. Issa, A.M.A. Henaish, Emad M. Ahmed, Y.S. Rammah, Fabrication, physical, structure characteristics, neutron and radiation shielding capacity of high-density neodymio-cadmium lead-borate glasses: Nd_2O_3/CdO/PbO/B_2O_3/Na_2O, Appl. Phys. A 128 (2022) 551, https://doi.org/10.1007/s00339-022-05689-5.

[16] S. Sankaran, R. Ehsani, Introduction to the electromagnetic spectrum. In Imaging with Electromagnetic Spectrum, Springer,, Berlin, Heidelberg, 2014, pp. 1–15.

[17] S.R. Adhikari, Effect and application of ionization radiation (X-Ray) in living organism, Himalayan Phys. 3 (2012) 89–92.

[18] Abdelhamid H. Elgazzar, Nafisa Kazem, "Biological effects of ionizing radiation, Pathophysiol. basis Nucl. Med. Springe Int. Publ. (2015) 715–726.

[19] I.C.R.P. International Commission on Radiological Protection 2009 Annual Report (2009).

[20] H.U. Chiegwu, D.C. Ugwuanyi, M.C. Okeji, E. Onwugalu, How Effic. are Lead. aprons Use Radiat. Prot. our Hosp. ?, Indian J. Appl. Res. 8 (2) (2018).

[21] M.M. Abuzaid, G. Susoy, S.A. Issa, W. Elshami, O. Kilicoglu, H.O. Tekin, Relationship between melting-conditions and gamma shielding performance of fluoro-sulfo-phosphate (FPS) glass systems: a comparative investigation, Ceram. Int. 46 (10) (2020) 15255–15269.

[22] W. Elshami, H.O. Tekin, M.S. Al-Buriahi, H.H. Hegazy, M.M. Abuzaid, S.A. Issa, H.M. Zakaly, Developed selenium dioxide-based ceramics for advanced shielding applications: Au2O3 impact on nuclear radiation attenuation, Results Phys. 24 (2021), 104099.

[23] G. ALMisned, W. Elshami, S.A. Issa, G. Susoy, H.M. Zakaly, M. Algethami, Y.S. Rammah, A. Ene, S.A. Al-Ghamdi, A.A. Ibraheem, H.O. Tekin, Enhancement of gamma-ray shielding properties in cobalt-doped heavy metal borate glasses: the role of lanthanum oxide reinforcement, Materials 14 (24) (2021) 7703.

[24] Y.S. Rammah, Zakaly, M.H. Hesham, Issa, A.M. Shams, H.O. Tekin, M.M. Hessien, H.A. Saudi, A.M.A. Henaish, Fabrication, physical, structural, and optical investigation of cadmium lead-borate glasses doped with Nd3+ ions: an experimental study, J. Mater. Sci: Mater. Electron 33 (2022) 1877–1887, https://doi.org/10.1007/s10854-021-07387-z.

[25] H.H. Hegazy, M.S. Al-Buriahi, F. Alresheedi, F.I. El-Agawany, C. Sriwunkum, R. Neffati, Y.S. Rammah, Nuclear shielding properties of B2O3–Bi2O3–SrO glasses modified with Nd2O3: Theoretical and simulation studies, Ceram. Int. 47 (2021) 2772–2780, https://doi.org/10.1016/j.ceramint.2020.09.131.

[26] H.O. Tekin, G. ALMisned, G. Susoy, Ali, T. Fatema, D.S. Baykal, A. Ene, Issa, A.M. Shams, Y.S. Rammah, Zakaly, M.H. Hesham, Transmission factor (TF) behavior of Bi2O3–TeO2–Na2O–TiO2–ZnO glass system: a monte carlo simulation study, Sustainability 14 (2022) 2893, https://doi.org/10.3390/su14052893.

[27] Y. Al-Hadeethi, M.I. Sayyed, Y.S. Rammah, Fabrication, optical, structural and gamma radiation shielding characterizations of GeO2-PbO-Al2O3–CaO glasses, Ceram. Int. 46 (2020) 2055–2062, https://doi.org/10.1016/j.ceramint.2019.09.185.

[28] M. Kasprzyk, M. Środa, M. Szumera, Influence of Gd_2O_3 on thermal stability of oxyfluoride glasses, J. Therm. Anal. Calor. 130 (2017) 207–220, https://doi.org/10.1007/s10973-017-6354-9.

[29] Y. Al-Hadeethi, M.I. Sayyed, J. Kaewkhao, et al., Physical, structural, optical, and radiation shielding properties of B2O3–Gd2O3–Y2O3 glass system, Appl. Phys. A 125 (2019) 852, https://doi.org/10.1007/s00339-019-3115-6.
[30] E. Kaewnuam, N. Wantana, S. Tanusilp, K. Kurosaki, P. Limkitjaroenporn, J. Kaewkhao, The influence of Gd2O3 on shielding, thermal and luminescence properties of WO3–Gd2O3–B2O3 glass for radiation shielding and detection material, ISSN 0969-806X, Radiat. Phys. Chem. Volume 190 (2022), 109805, https://doi.org/10.1016/j.radphyschem.2021.109805.
[31] M. Almateri, O. Agar, E.E. Altunsoy, O. Kilicoglu, M.I. Sayyed, H.O. Tekin, Photon and neutron shielding characteristics of samarium doped lead alumino borate glasses containing barium, lithium and zinc oxides determined at medical diagnostic energies, Results Phys. 12 (2019) 2123–2128, https://doi.org/10.1016/j.rinp.2019.01.094.
[32] H.O. Tekin, G. ALMisned, G. Susoy, F.T. Ali, D.S. Baykal, A. Ene, S.A.M. Issa, Y.S. Rammah, H.M.H. Zakaly, Transmission Factor (TF) Behavior of Bi_2O_3–TeO_2–Na_2O–TiO_2–ZnO Glass System: A Monte Carlo Simulation Study, Sustainability 14 (2022) 2893, https://doi.org/10.3390/su1405289.
[33] H.O. Tekin, G. ALMisned, Y.S. Rammah, et al., The significant role of WO3 on high-dense BaO–P2O3 glasses: transmission factors and a comparative investigation using commercial and other types of shields, Appl. Phys. A 128 (2022) 470, https://doi.org/10.1007/s00339-022-05620-.
[34] M. Almateri, O. Agar, E.E. Altunsoy, O. Kilicoglu, M.I. Sayyed, H.O. Tekin, Photon and neutron shielding characteristics of samarium doped lead alumino borate glasses containing barium, lithium and zinc oxides determined at medical diagnostic energies, Res. Phys. 12 (2019) 2123–2128, https://doi.org/10.1016/j.rinp.2019.01.094.
[35] E. Şakar, Ö.F. Özpolat, B. Alım, M.I. Sayyed, M. Kurudirek, Phy-X / PSD: development of a user friendly online software for calculation of parameters relevant to radiation shielding and dosimetry, Radiat. Phys. Chem. 166 (2020), 108496.
[36] RSICC Computer Code Collection, MCNPX 'User's Manual Version 2.4.0. Monte Carlo N-Particle Transport Code System for Multiple and High Energy Applications; 2002.